

Article

New Carriers for Bioadhesive Gastroretentive Drug Delivery Systems Based on Eudragit[®] EPO/Eudragit[®] L100 Interpolyelectrolyte Complexes

Daria S. Gordeeva, Aleksandra V. Sitenkova (Bukhovets) and Rouslan I. Moustafine * 

Institute of Pharmacy, Kazan State Medical University, 16 Fatykh Amirkhan Street, Kazan 420126, Russia; daria.gordeeva@kazangmu.ru (D.S.G.); aleksandra.sitenkova@kazangmu.ru (A.V.S.)

* Correspondence: ruslan.mustafin@kazangmu.ru; Tel.: +7-843-252-1642

Abstract: The aim of this study was the analysis of interpolyelectrolyte complexes (IPECs) based on Eudragit[®] EPO and Eudragit[®] L100 as prospective carriers for gastroretentive drug delivery systems (GRDDS) using two model drugs: metronidazole (MZ) and acyclovir (ACR). Eudragit[®] EPO/L100 IPECs with different pH concentrations were characterized by different degrees of swelling in mimicking fasted stomach medium (0.1 M HCl) and saved their shape for 6 h. The microenvironmental changes in IPEC structures in acidic medium were investigated using FT-IR spectroscopy, thermal and elemental analysis. IPEC samples showed bioadhesive properties that were not significantly different from the positive control (Carbopol) in the test with the mucin compacts. The release rate of metronidazole (class I BCS) from IPEC matrices increased with the increasing degree of swelling. IPEC 1 provided $49.62 \pm 6.20\%$ and IPEC 2 reached $87.69 \pm 5.15\%$ of metronidazole release after 6 h in mimicking fasted stomach medium (0.1 M HCl). The total amount of released acyclovir (class III BCS) from IPEC 1 was $25.76 \pm 5.67\%$ and from IPEC 2 was $21.48 \pm 5.00\%$. Release of both drugs was controlled by relaxation of polymeric chains in matrices according to the Peppas–Sahlin model. According to the received results, investigated interpolymer complexes are prospects for further evaluation as carriers for gastroretentive bioadhesive systems.



Citation: Gordeeva, D.S.; Sitenkova, A.V.; Moustafine, R.I. New Carriers for Bioadhesive Gastroretentive Drug Delivery Systems Based on Eudragit[®] EPO/Eudragit[®] L100 Interpolyelectrolyte Complexes. *Sci. Pharm.* **2024**, *92*, 14. <https://doi.org/10.3390/scipharm92010014>

Academic Editor: Nilesh Patel

Received: 18 December 2023

Revised: 22 January 2024

Accepted: 17 February 2024

Published: 22 February 2024

Keywords: interpolyelectrolyte complexes; Eudragit[®]; gastroretentive systems; drug delivery systems; bioadhesive systems; metronidazole; acyclovir

1. Introduction

Gastroretentive drug delivery systems (GRDDS) are used for site-specific drug release and systematic action in the upper part of the gastrointestinal tract (GIT), especially for the drugs with an absorption window in the proximal small intestine [1,2] and local action for treatment of the inflammatory or cancerous diseases and eradication of *Helicobacter pylori* [3,4]. There are several technologies to achieve increasing drug residence in the upper part of the GIT, such as magnetic systems [5], mucoadhesive systems [6,7], expandable systems [8], floating systems [9,10], high-density systems [11,12] and polymeric fibrous materials [13,14].

Bioadhesive gastroretentive drug delivery systems are on the way to prolong the drug residence time in the upper part of the GIT. It is known that polymers for bioadhesive systems include hydrogen-bond-forming groups, such as carboxyl, hydroxyl, amide and sulfate groups. Bioadhesive GRDDS action is based on a complex process with several mechanisms, including electrical theory, adsorption, wetting, diffusion and fracture theories [15,16]. Bioadhesive polymers such as Carbopol[®], chitosan, hydroxypropyl methylcellulose (HPMC) and sodium carboxymethyl cellulose (CMC-Na) are usually used for such type of GRDDS [17–19]. However, several polymer excipients must be used to ensure the required gastroretentive effect. For example, Naseem et al. Developed gastroretentive formulations consisting of osmotically controlled polymer, hydrophilic polymer, hydrophilic



Copyright: © 2024 by the authors. Licensee MDPI, Basel, Switzerland. This article is an open access article distributed under the terms and conditions of the Creative Commons Attribution (CC BY) license (<https://creativecommons.org/licenses/by/4.0/>).

gums, gel-forming polymers and mucoadhesive polymers with microcrystalline cellulose [6]. Zhu et al. provided results of an assessment of bioadhesive gastroretentive minitables containing HPMC, Carbopol® 971P, microcrystalline cellulose and aerosil [17]. Development of gastroadhesive matrix systems based on a combination of Eudragit® E100, CMC-Na and locust bean gum was reported by Ngwuluka et al. [20]. This study was focused on developing a gastroretentive drug delivery system employing a triple-mechanism interpolymeric blend matrix comprising high density, swelling and bioadhesiveness for the enhanced site-specific zero-order delivery of levodopa in Parkinson's disease.

The combination of oppositely charged types of methacrylate copolymers, including their blends, in order to control the site and time of drug release from oral drug delivery systems (DDS) was discussed in previously published reviews [21,22]. A comprehensive analysis of the physico-chemical principles of the intermacromolecular interactions in oral DDS, based on chemically complementary Eudragit®-grade copolymers, was published by our research group [23,24].

Investigation of the interpolyelectrolyte complexes (IPEC) based on oppositely charged Eudragit® copolymers have been actively carried out over the last fifteen years [25–37]. The main reason for this fact is the structure of (meth)acrylate copolymers; Eudragits contain oppositely charged groups, from which reaction of polycomplex formation is possible.

Initially, the influence of the combination of two oppositely charged polymers, Eudragit® EPO (EPO) and Eudragit® L100 (L100), was studied for oral controlled DDS [26]. These grades were combined in the polycomplex matrix system because of their hydrophilic–hydrophobic properties that could be suitable in colon-specific controlled DDS. The combination of two pH-dependent copolymers EPO/L100 at the necessary molar ratio can provide the required diffusion transport properties and controlled drug release. FTIR analysis indicated that samples were not stable in a strongly acidic gastric-mimicking medium. However, swelling testing of the polycomplex systems using gastric-mimicking conditions showed that all IPEC samples were characterized by an unexpected stability within the strongly acidic medium in spite of the destroying of ionic bonds.

Thus, taking into account our results, we decided to follow this interesting idea and do additional experiments focused on finding prospective bioadhesive IPEC samples for the development of sustained gastroretentive drug delivery polyelectrolyte matrix based on oppositely charged Eudragit® EPO and Eudragit® L100 [38].

It is also known that IPECs contain ionized groups of the individual polymers in the defective areas of their structure and, therefore, using IPEC can provide bioadhesive effects for drug delivery systems [39,40].

Moreover, we have established that EPO exhibits mucoadhesive properties and retains the dye on the mucosal surface better compared to free sodium fluorescein. This good retention of the dye mediated with EPO on mucosal surfaces is likely to be related to its cationic nature, which ensures electrostatic attraction of this polymer to the negatively charged mucosal surface [41].

Recently, we have also reported that better retention properties of IPECs based on Eudragit® EPO/Eudragit® L100-55 copolymers compared to pure EPO is possibly related to their insoluble nature and slower elimination from the mucosal surface [42].

The aim of this study was the analysis of two IPECs based on Eudragit® EPO and Eudragit® L100, previously chosen as prospective carriers for GRDDS by additional evaluating of swelling, bioadhesiveness and release properties for the enhanced gastro-specific delivery for two model drugs: metronidazole (MZ) and acyclovir (ACR).

The main absorption site of ACR is the upper part of GIT. Moreover, it has a short half-life of approximately 2.5 h [43]. Therefore, development of GRDDS of ACR may improve its bioavailability.

On the other hand, MZ is an antibacterial drug that is used for treatment of chronic bacterial infection caused by *Helicobacter pylori* and plays an important role in the development of peptic ulcers and gastric carcinoma [44]. Development of a dosage form of MZ

with localized action in the stomach can also help in solving the problem of increasing effectiveness of pharmacotherapy of these diseases.

2. Materials and Methods

2.1. Materials

EPO is a polycation, terpolymer of dimethylamino-ethyl methacrylate with methyl methacrylate and butyl methacrylate (mole ratio 2:1:1, MW 150,000 g/mol), L100 is polyanion, copolymer of methacrylic acid and methyl methacrylate (mole ratio 1:1, MW 135,000 g/mol), which were used for preparation of IPECs and physical mixtures (PhM). These copolymers were generously provided by Evonik Industries AG (Darmstadt, Germany). MZ and ACR were purchased from Merck (Sigma-Aldrich, St. Louis, MO, USA). Mucin isolated from pig stomachs (type II) (Merck group, Sigma-Aldrich, St. Louis, MO, USA) and fragments of the pig stomach mucosa were used to study bioadhesive properties.

Sodium hydroxide (NaOH), reagent grade, $\geq 98\%$, pellets (anhydrous) (Sigma-Aldrich, St. Louis, MO, USA) and hydrochloric acid (HCl), 36.5–38.0% (Sigma-Aldrich, St. Louis, MO, USA) were used for the preparation 1 M solutions for pH adjusting. Hydrochloric acid (HCl), 36.5–38.0% (Sigma-Aldrich, St. Louis, MO, USA), was used for preparation of a 0.1 M solution to simulate the fasted stomach.

2.2. Preparation of Solid Interpolyelectrolyte Complexes (IPEC) and Physical Mixtures (PhM)

Preparation of solid IPECs based on Eudragit[®] copolymers was carried out in an aqueous solution under pH 6.0 (IPEC 1) and pH 6.5 (IPEC 2). Solutions of EPO and L100 were prepared separately, adjusted to the necessary pH and mixed as it was described earlier [26]. The powders of vacuum-dried (vacuum oven VD 23, Binder GmbH, Tuttlingen, Germany) IPEC samples were previously ground using an automatic accessory for mixing and grinding ShakIR (Pike Technologies, Madison, WI, USA) before pressing them into the matrices.

PhMs were prepared by mixing powders of copolymers EPO and L100 using an automatic accessory for mixing and grinding ShakIR (Pike Technologies, Madison, WI, USA).

2.3. Preparation of Tablets

Matrices of IPEC and PhM for studying swelling ability (100 mg, 8 mm in diameter), were obtained by pressing on a PressPRO 15-ton programmable automated hydraulic press for IR spectroscopy (Pike Technologies, Madison, WI, USA) at a pressure of 2.45 MPa.

Tablets for analysis of drug release contained a mixture of IPEC or PhM (50 mg) and model drug (100 mg), 8 mm in diameter, which were pressed on a PressPRO 15-ton programmable automated hydraulic press for IR spectroscopy (Pike Technologies, Madison, WI, USA) at a pressure of 2.45 MPa.

2.4. Determination of the Degree of Swelling of Matrices

The study of the swelling ability was carried out in mimicking fasted stomach medium (0.1 M HCl) at a temperature of 37 ± 0.5 °C for 6 h. The polymeric matrix was placed in a tared basket, which was immersed into a thermostatic bath IC control eco 18c (IKA[®] Werke GmbH, Staufen, Germany). The total volume of the medium was 40 mL. The basket was removed from the medium every 30 min and the matrix was carefully dried using a filter paper and weighed.

The degree of swelling ($H\%$) was calculated by the formula:

$$H\% = ((m_2 - m_1)/m_1) \cdot 100, \quad (1)$$

in which m_1 is the mass of the dry sample; m_2 is mass of swollen sample.

2.5. Elemental Analysis

The compositions of the IPEC samples and IPEC samples after swelling assessment were investigated by elemental analysis using a CHNS/O Elemental Analyzer Thermo Flash 2000 (Thermo Fisher Scientific, Paisley, UK) and calculated as $Z = [\text{EPO}]:[\text{L100}]$ (mol/mol). The vacuum-dried samples (at 40 °C for 2 days) were weighed into a crucible on a XP6 Excellence Plus XP micro balance (Mettler Toledo, Greifensee, Switzerland). The crucibles with samples were packed and placed into the combustion reactor via autosampler. Temperature in the oven was 900 °C, a gas flow rate was 10 mL/min. Calibration of the instrument was performed with atropine standard (Thermo Fisher Scientific, Paisley, UK). Eager Xperience Data Handling Software (version 1.3.07/2014) was used to analyze the results. All measurements were performed in triplicate.

The content of nitrogen (%) was taken into account. Only EPO contains nitrogen. The compositions of the IPEC samples were calculated, taking into account molar masses of the initial copolymer units and the percentage of nitrogen in each sample.

2.6. Fourier-Transformed Infrared (ATR-FTIR) Spectroscopy

ATR-FTIR spectra were recorded by a Nicolet iS5 FTIR spectrometer (Thermo Scientific, Waltham, MA, USA) using the iD5 smart single bounce ZnSe ATR crystal. The spectra were analyzed using OMNIC spectra software (version 8.2.387).

2.7. Thermal Analysis

Modulated DSC (mDSC) measurements were carried out using a Discovery DSC™ (TA Instruments, New Castle, DE, USA), equipped with a refrigerated cooling system (RCS90). TRIOS™ software (version 3.1.5.3696) was used to analyze the DSC data (TA Instruments, New Castle, DE, USA). Tzero aluminum pans (TA Instruments, New Castle, DE, USA) were used in all calorimetric studies. The empty pan was used as a reference and the mass of the reference pan and of the sample pans were taken into account. Dry nitrogen was used as a purge gas through the DSC cell at 50 mL/min. Indium and n-octadecane standards were used to calibrate the DSC temperature scale; enthalpic response was calibrated with indium. Calibration of heat capacity was done using sapphire. Initially, the samples were cooled from room temperature to 0 °C, then kept at 0 °C for 5 min and analyzed from 0 to 250 °C. The heating rate was 2 °C/min with a 40 s period and 1 °C amplitude. Glass transition temperatures were determined using the reversing heat flow signals. All measurements were performed in triplicate.

2.8. Study of Model Drug Release

The study of the release of MZ and ACR from tablets based on the IPECs and PhMs was carried out using the Flow-Through Cell Apparatus on a CE 7 Smart device (Sotax AG, Aesch, Switzerland), mimicking fasted stomach medium (0.1 M HCl; 37 ± 0.5 °C), at a biorelevant flow rate of 8 mL/min in an open cycle [37] for 6 h. The amount of released MZ and ACR were estimated by UV spectrophotometer Evolution 220 (Thermo Scientific, Waltham, MA, USA) at a wavelength of 274 nm (MZ) and 202 nm (ACR), respectively. The concentration of drugs in the release medium was calculated based on calibration curves. Release profiles were fitted using Microsoft Excel Office software 2021 MSO (Version 2401 Build 16.0.17231.20236) according to the zero-order, first-order and Peppas–Sahlin models [45,46].

2.9. Analysis of Bioadhesive Properties

IPEC and PhM adhesion was studied on a TA.XTplus texture analyzer (Stable Micro Systems, Surrey, UK). Mucin compacts and fragments of the pig stomach mucosa were used as substrates for adhesion. Mucin compacts were obtained by pressing on a 15-ton microprocessor-controlled automated hydraulic press for IR spectroscopy (Pike Technologies, Madison, WI, USA) at a pressure of 2.45 MPa using 13 mm die for IR spectroscopy (Pike Technologies, Madison, WI, USA). Pig stomach tissue was received from an abattoir

immediately after animal slaughter and transferred in a polystyrene container with dry ice. Stomach tissues were defrosted and excised to 3×3 cm sections. Bioadhesive properties on the pig stomach mucosa were studied in the acidic medium (0.1 M HCl). IPEC or PhM compacts were attached to the probe, while mucin compacts or stomach tissue were placed on the platform. Carbopol® 2020 (Carbopol) was used as a reference (positive control). The parameter settings of analysis with mucin compacts were [20]: pre-test speed (0.5 mm/s), test speed (0.1 mm/sec), post-test speed (0.1 mm/s), applied force (0.1 N), trigger force (0.1 N), return distance (10 mm). The parameter settings of analysis with pig stomach tissue were: pre-test speed (1 mm/s), test speed (0.1 mm/sec), post-test speed (0.1 mm/s), applied force (0.1 N), trigger force (0.1 N), return distance (10 mm). The residence time of each formulation on the mucin compact and pig stomach mucous membrane was 60 s. The data were captured through Texture Exponent Software (Version 3.2). The peak force was used to assess the gastroadhesivity of the matrices. The peak force is the maximum force required to detach the membrane or the tissue from the matrices [20].

2.10. Statistical Analysis

All experiments were carried out in triplicate. Microsoft Excel Office software 2021 MSO (Version 2401 Build 16.0.17231.20236) was used for statistical analysis. Mean values \pm standard deviations were calculated using one-way analysis of variance (ANOVA) and *t*-Test (Two-Sample Assuming Equal Variances), where probability was $p < 0.05$ as a significant criterion.

3. Results and Discussion

3.1. Composition Study

Compositional differences of the synthesized IPECs were observed using elemental analysis (Table 1). The fraction of polycation (EPO) incorporated in the polycomplex increased as the pH of the reaction medium rose. IPEC 1 (synthesized at pH 6.0) had a composition close to equimolar ($Z = [\text{EPO}]/[\text{L100}] = 1.02$). IPEC 2 (synthesized at pH 6.5) contained a 1.5-fold excess of EPO ($Z = 1.49$). Thus, the polycomplexes were enriched with the less ionized component (EPO) – IPEC 2.

Table 1. Characteristics of IPEC EPO/L100 systems.

Sample Symbol	pH at Which IPEC Was Obtained	IPEC Composition		Tg Value, °C
		$Z = [\text{EPO}]/[\text{L100}]$	EPO:L100 (mol/mol)	
IPEC 1	6.0	1.02	1:0.98	146.6 ± 0.3
IPEC 2	6.5	1.49	1:0.67	117.4 ± 0.2

Eudragit copolymers are amorphous substances and have a characteristic glass transition temperature (Tg) [21,23]. mDSC was used to confirm the structural differences between prepared IPECs, as well as to evaluate the chemical homogeneity of the polymer systems by the absence of microdomains of free copolymers. Both IPECs were characterized by the presence of one Tg, which was higher than for EPO (52.1 ± 1.3 °C) but lower than for L100 (193.3 ± 1.8 °C).

3.2. Assessment of the IPEC Behavior in Acidic Medium

Assessment of the behavior of IPEC matrices without drugs in mimicking biological liquids media is necessary for prediction of the possibility of application of IPEC as carriers for DDS. The behavior of matrices based on IPEC Eudragit® EPO/L100 in comparison with matrices based on PhMs was investigated under the conditions mimicking medium of the fasted stomach (0.1 M HCl). It was noted that matrices based on PhMs dissolved after 2 h in an acidic medium. Matrices based on IPECs retained their shape, increased in size and transformed into a hydrogel structure that withstood the entire 6 h of the experiment

(Figure 1). Based on the comparison of swelling profiles (Figure 2), it can be concluded that matrices of IPEC 2 were characterized by slower increase of the degree of swelling in the first hours of exposure to the medium. However, the degree of swelling of the matrix based on IPEC 2 was higher (851.53%) than that of IPEC 1 (481.54%) by the end of the experiment.

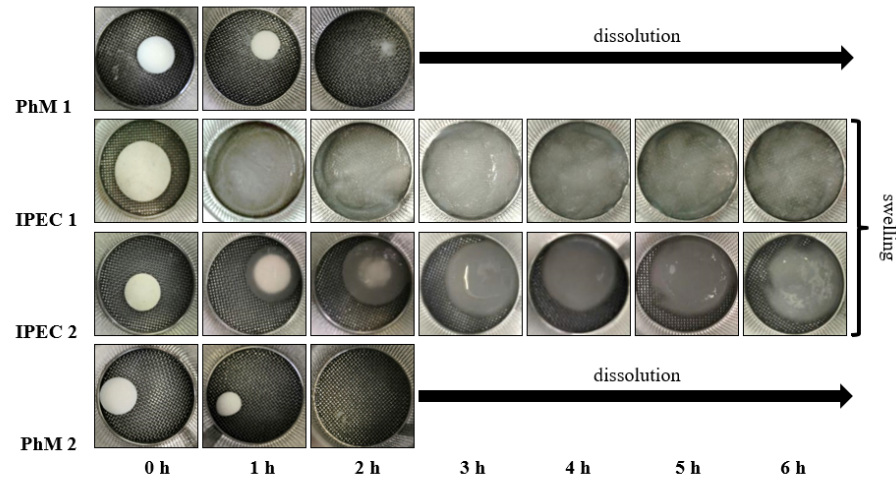


Figure 1. External appearance of IPEC and PhM matrices during the swelling test.

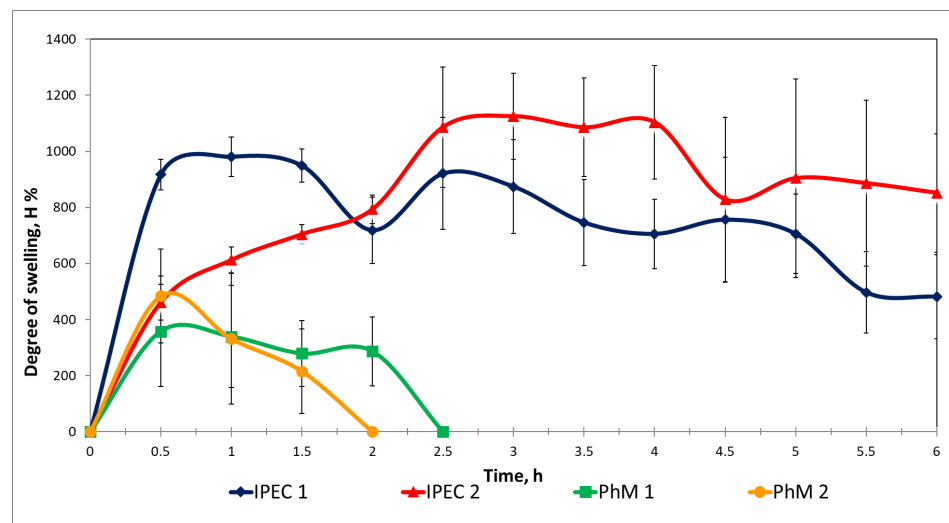


Figure 2. Swelling profiles of IPEC and PhM matrices in mimicking fasted stomach medium (0.1 M HCl) ($n = 3$, mean \pm SD).

The different behavior of matrices based on PhMs and IPECs is most likely explained by the structure of IPEC stabilized by intermacromolecular ionic bonds between ionized dimethylamino groups of EPO and carboxylate groups of L100. The presence of these bonds has been proven by a new characteristic band at 1560 cm^{-1} in the FTIR spectrum of IPECs. The FTIR spectra (Figures 3 and 4) of the obtained IPEC 1 and IPEC 2 show that the intensity of the characteristic band at 1560 cm^{-1} decreased with an increasing residence time of the IPEC matrices in mimicking fasted stomach medium (0.1 M HCl). This fact can explain slight dissolution of matrices, which led to a decrease in the swelling plot.

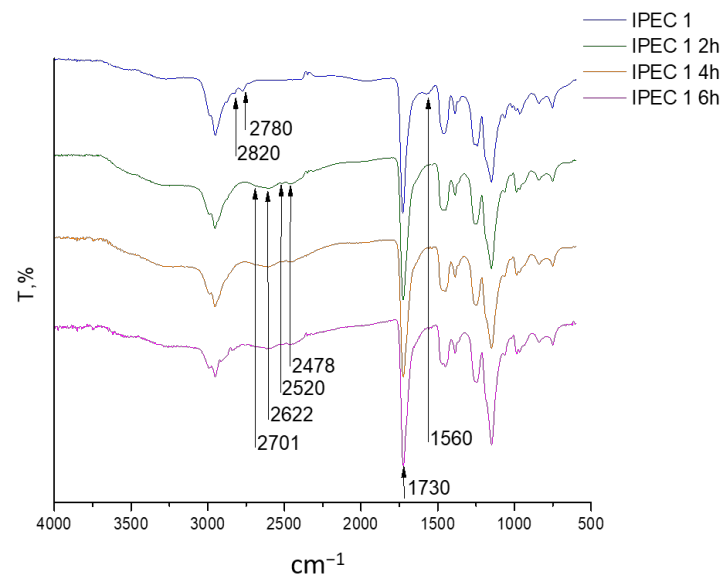


Figure 3. FTIR-spectra of IPEC 1 after swelling in mimicking fasted stomach medium (0.1 M HCl).

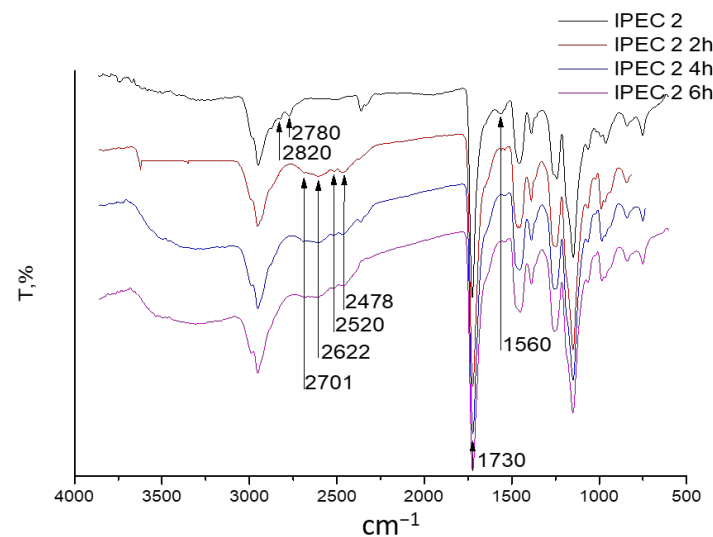


Figure 4. FTIR-spectra of IPEC 2 after swelling in mimicking fasted stomach medium (0.1 M HCl).

On the other hand, significant peak broadening at approximately $2520\text{--}2478\text{ cm}^{-1}$ can be assigned to the interpolymer absorption band, which resulted from hydrogen bonding interaction of the dimethylamino groups or the carbonyl of EPO with the hydroxyls from the carboxylic groups of L100. Another new wide band between 2350 and 2750 cm^{-1} in the IPECs spectrum indicates the occurrence of different dimeric and monomeric forms of the ammonium cation, which, in turn, may be associated with water molecules. This fact is consistent with our previous studies [26].

We applied mDSC to analyze the behavior of IPEC matrices while passing them through a fasted-stomach-mimicking medium. Immersion of the IPEC 1 matrices up to 6 h led to a sharp increase of the T_g from 117.4 ± 0.2 to $170.6 \pm 0.1\text{ }^\circ\text{C}$. Moreover, all mDSC thermograms showed only one T_g , which indicates that both IPECs were not disintegrated to individual copolymers due to the absence of microdomains of them.

Possible compositional changes of the synthesized IPECs were found using elemental analysis. Table 2 illustrates that the sample containing an excess of EPO (IPEC 2, $Z = 1.49$) lost a significant amount of polycation that caused compositional changes in the poly-complex. Thus, during testing, only one-third of the EPO was retained relative to L100

($Z = 0.5$). In case of the equimolar sample (IPEC 1), there were similar compositional and structural changes, but with less leaching of EPO from the polycomplex matrix. Comparative analysis of the T_g values indicated that the process of EPO leaching during residence in the mimicking fasted stomach medium correlated with the compositional changes of the tested polycomplex system and concurred with previously published results [26]. Thermograms are presented on Figures S1–S6.

Table 2. Results of the thermal and elemental analysis for IPEC samples after swelling in mimicking fasted stomach medium (0.1 M HCl) ($n = 3$, mean \pm SD).

	Glass Transition, °C	Elemental Analysis	
	T_g	Composition $Z = \text{EPO:L100 (mol/mol)}$	N, %
IPEC 1–2 h	165.8 \pm 0.1	1:1.17	2.84 \pm 0.16
IPEC 1–4 h	170.7 \pm 0.1	1:1.11	2.91 \pm 0.26
IPEC 1–6 h	170.6 \pm 0.1	1:1.08	3.11 \pm 0.10
IPEC 2–2 h	169.5 \pm 0.1	1:1.22	2.78 \pm 0.11
IPEC 2–4 h	172.3 \pm 0.5	1:1.47	2.54 \pm 0.12
IPEC 2–6 h	173.9 \pm 0.3	1:1.27	2.75 \pm 0.31

According to the received swelling assessment results, such intrastructural processes that occur with IPEC matrices were not a limiting factor and allowed the matrices to stay in an acidic mimicking fasted stomach medium for 6 h. It may indicate the prospects for further studies of IPEC data as carriers for GRDDS.

3.3. Analysis of Bioadhesive Properties

There are two stages in the adhesion process: contact and consolidation. In the first stage, contact between tablet and mucosa happens and the polymer swells and melts. There is a bond formation between the polymer and mucin in the second stage [20,47].

In the bioadhesive properties study, there was a difference in mucoadhesion using mucin compacts and mucosa tissue. Mucin compacts can be used for checking the ability to adhere on the mucosa but they do not imitate a real tissue properly, as we proved. The contact of the tablet and mucin compact is tight, and there is a high experimental reproducibility. Adhesion of Carbopol (positive control) was found not to be significantly different from IPECs and PhMs. Results of studying peak positive force of tablets on mucin compacts are shown on Figure 5.

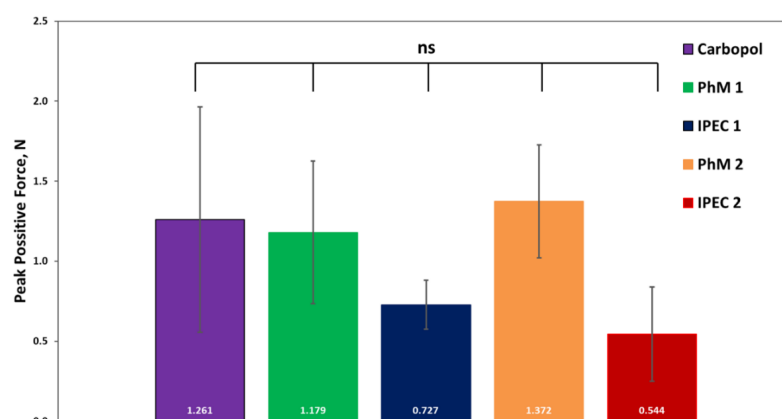


Figure 5. Results of measuring peak positive force of IPECs and PhMs from mucin compacts (N) ($n = 3$, mean \pm SD, “ns” represents not significant).

We proved that PhMs and IPECs have high mucoadhesive properties as Carbopol. We repeated the adhesion test using pig stomach tissue. Figure 6 shows peak positive force results on pig stomach mucosa. The adhesion on the mucosa tissue depends on different factors: contact surface, hydration, part of the stomach, etc. Carbopol had a better adhesion on stomach mucosa than IPECs and PhMs. But in case of excessive adhesive properties of gastroretentive systems, they can be adhesive to the throat or esophagus and cause damage [47].

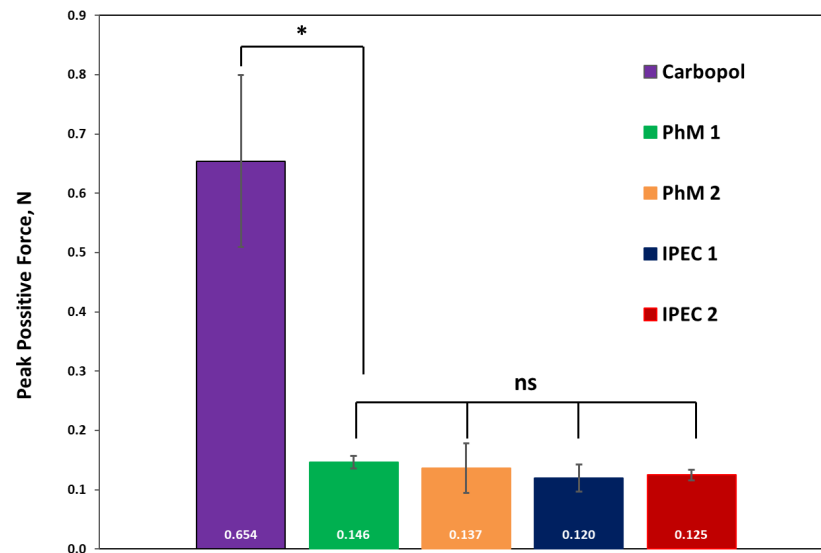


Figure 6. Results of measuring peak positive force of IPECs and PhMs from pig stomach mucosa (N) ($n = 3$, mean \pm SD, “*” represents $p < 0.05$, “ns” represents not significant).

3.4. Study of Drug Release

MZ and ACR are both characterized by high solubility in bioliquids of gastrointestinal tract. MZ is a class I type of drug according to the biopharmaceutical classification system (BCS) [48,49]. ACR is a class III type drug of BCS [50,51].

According to the received results (Figure 7), release profiles of MZ had similar characteristics for all samples, with the total amount of released drug more than $49.62 \pm 6.20\%$ for matrices based on IPEC 1 and $87.69 \pm 5.15\%$ for matrices based on IPEC 2. The amount of released MZ from both PhMs was around 50%. These results are consistent with previously published data regarding theophylline, which has good solubility in biological fluids of the GIT and belongs to the I class of BCS [26]. The release rate of MZ increased with the increasing degree of swelling. The slightly different shape of the IPEC 2 curve is associated with the disintegration of the matrix that occurred during the experiment.

Matrices based on PhMs provided 20% lower release of ACR to the acidic medium after 6 h (Figure 8). Total amount of released ACR from IPEC 1 was $25.76 \pm 5.67\%$ and from IPEC 2 was $21.48 \pm 5.00\%$. Despite the close values of the ACR concentration in the dissolution medium to the end of the experiment, the profiles were different for matrices based on IPEC 1 and IPEC 2. IPEC 2 provided fast release of ACR for 1 h, with the subsequent drug concentration reaching the plateau. Release profile of ACR from IPEC 1 matrices can be characterized as prolonged with gradual drug release over 6 h.

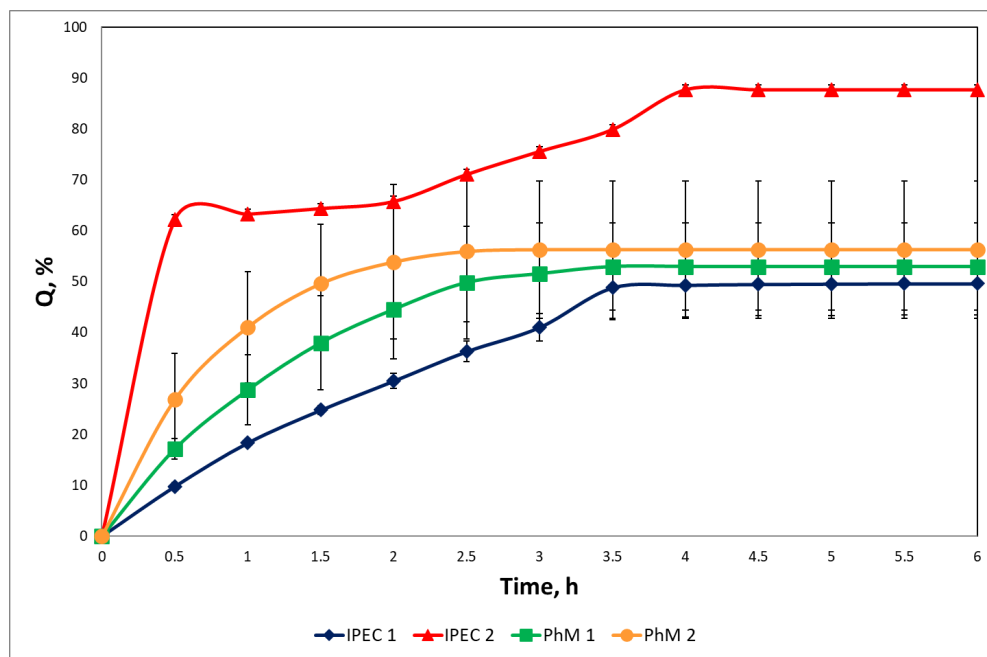


Figure 7. Release profiles of metronidazole from IPEC and PhM matrices in mimicking fasted stomach medium (0.1 M HCl) ($n = 3$, mean \pm SD).

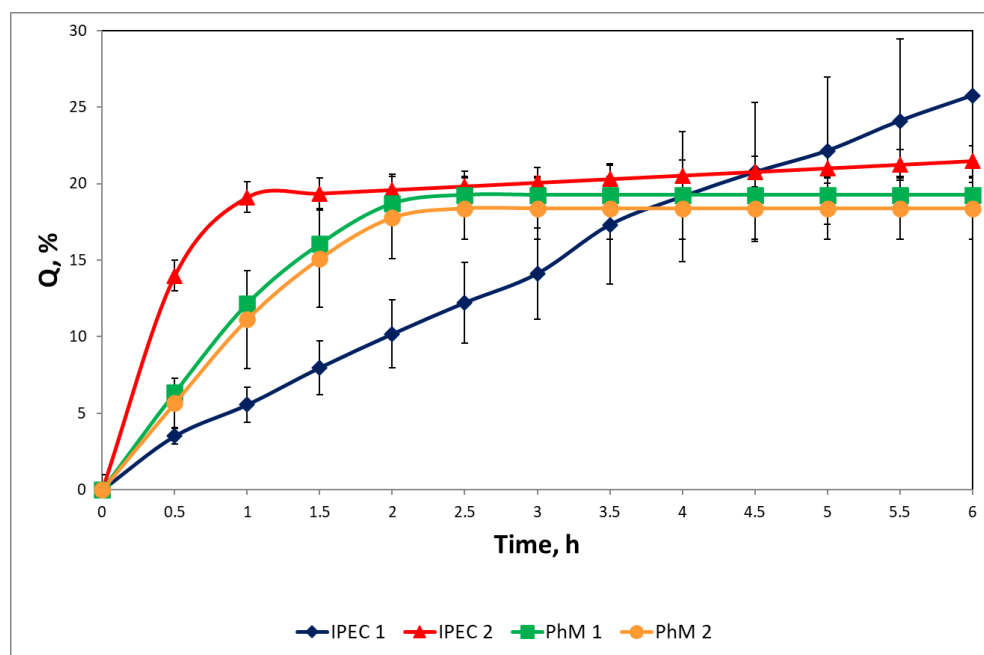


Figure 8. Release profiles of acyclovir from IPEC and PhM matrices in mimicking fasted stomach medium (0.1 M HCl) ($n = 3$, mean \pm SD).

Release data were fitted according to the zero-order, first-order and Peppas–Sahlin equations to understand the mechanisms underlying the release of the MZ and ACR from polycomplex matrix systems. Data are presented in Tables 3 and 4.

Table 3. Results obtained from fitting experimental MZ release data.

Sample	Model	R ²
IPEC 1	Zero-order	0.5952
	First-order	0.8459
	Peppas–Sahlin	0.9762

Table 4. Results obtained from fitting experimental ACR release data.

Sample	Model	R ²
IPEC 1	Zero-order	−17.3238
	First-order	0.9935
	Peppas–Sahlin	0.9813
IPEC 2	Zero-order	−17.3238
	First-order	−15.0387
	Peppas–Sahlin	0.9892

According to the received results using a zero-order model is not suitable for describing the mechanism of MZ and ACR release from polycomplex matrix systems. Only release of ACR from IPEC 1 matrices can be correctly described according to the first-order model, whereas, according the received values of R², the Peppas–Sahlin equation could be used for understanding the mechanisms of model drug release from the investigated samples.

The Peppas–Sahlin Equation (2) takes into account the interrelated effects of Fickian diffusion and Case II transport.

$$Q = K_1 \cdot t^m + K_2 \cdot t^{2m} \tag{2}$$

where Q is the fraction of the drug released at time t, K₁ and K₂ are kinetic constants, m is diffusional exponent.

The K₁ value demonstrates the contribution of Fickian diffusion, while the K₂ value is related with both dissolution and relaxation of polymers chains [52].

Tables 5 and 6 and Figures 9 and 10 show the Peppas–Sahlin model experimental data analysis. Release of MZ from IPEC 2 exceeded 60% after the first hour; therefore, data are not provided.

Table 5. Results obtained from fitting experimental MZ release data to the Peppas–Sahlin model.

Parameters	IPEC 1
m	0.2681
K ₁	0.1000
K ₂	2.3675
R ²	0.9762

Table 6. Results obtained from fitting experimental ACR release data to the Peppas–Sahlin model.

Parameters	IPEC 1	IPEC 2
m	0.2681	0.0605
K ₁	0.1000	0.1675
K ₂	2.3676	10.5505
R ²	0.9813	0.9892

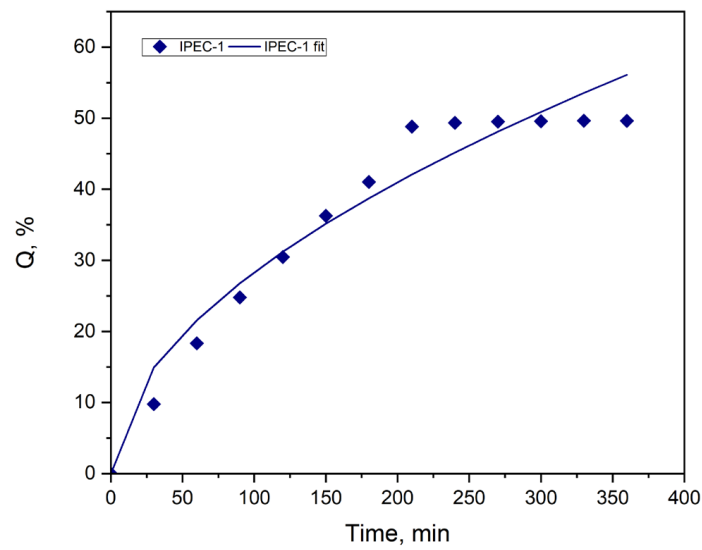


Figure 9. Release of MZ from matrix based on IPEC 1 in mimicking fasted stomach medium (0.1 M HCl). Experimental data points and predicted data from the Peppas–Sahlin model.

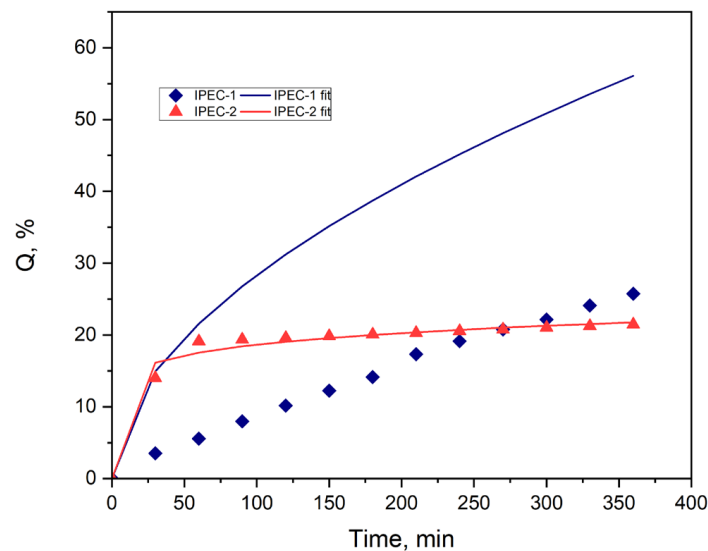


Figure 10. Release of ACR from matrix based on IPEC 1 and IPEC 2 in mimicking fasted stomach medium (0.1 M HCl). Experimental data points and predicted data from the Peppas–Sahlin model.

According to the value of R^2 , the Peppas–Sahlin model may be taken into consideration for explanation of the drug release mechanism.

Relaxation contribution/Fickian contribution (R/F) ratio was calculated by using the received parameters (Figures 11 and 12). $R/F > 1$ for both complexes with MZ and ACR, which showed that the erosion dominates during the process of both drug releases. The drug releases for MZ and ACR are controlled by relaxation of polymeric chains in matrices. That is, increasing R/F ratio values for release MZ in ACR from IPEC 1 matrices with time indicates the increasing relaxational contribution [53].

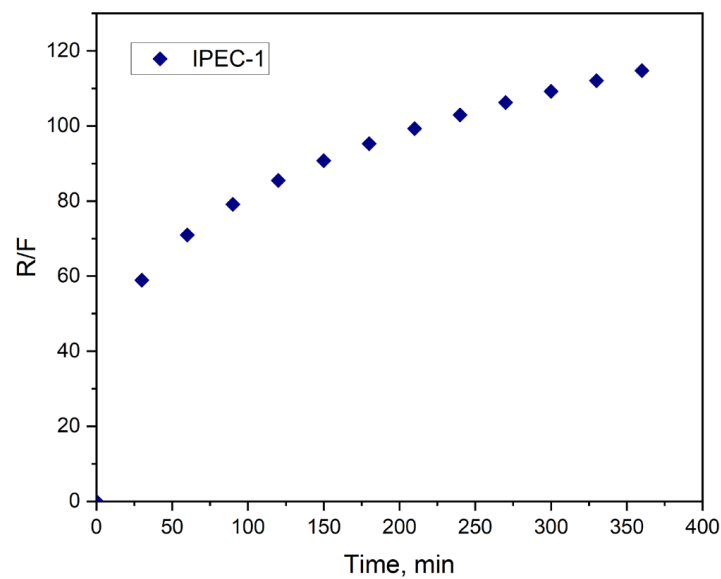


Figure 11. Relaxation contribution (R)/Fickian contribution (F) ratio with respect to time for metronidazole release.

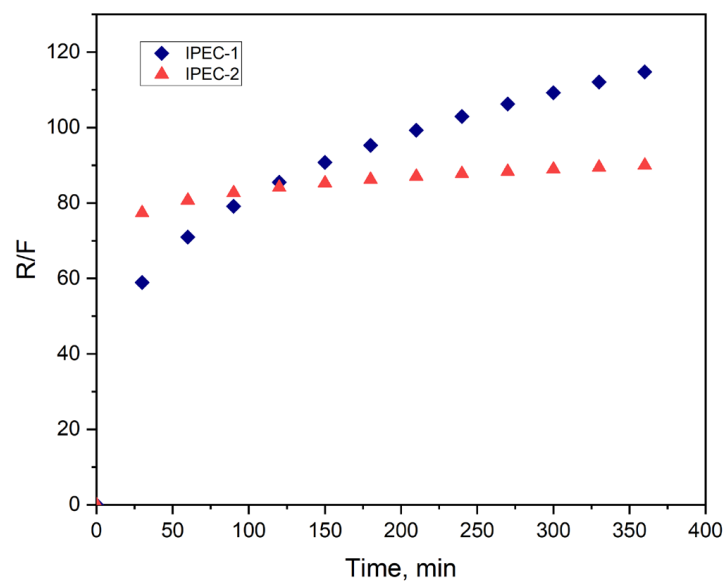


Figure 12. Relaxation contribution (R)/Fickian contribution (F) ratio with respect to time for acyclovir release.

4. Conclusions

Received results showed the potential of IPEC Eudragit® EPO/L100 as a controlled release carrier for gastroretentive delivery, due to comparable swelling properties in acidic medium mimicking fasted stomach and suitable bioadhesive properties. The assessment of possible structural and compositional differences in the formulation of polycomplexes during their stay in the tested media indicates that the analyzed samples are self-healing systems. Intrastructural processes that occurred with IPEC matrices were not a limiting factor and allowed the matrices to stay in an acidic medium.

The release rate of MZ (class I BCS) from IPEC matrices increased with the increasing degree of swelling. IPEC 1 provided prolonged release of MZ in mimicking fasted stomach medium (0.1 M HCl). Matrices based on both IPECs provided slow release of ACR (class III BCS) in acidic medium, with total amount of released drug less than 30% for the 6 h of the experiment. Release of both drugs was controlled by relaxation of polymeric chains in

matrices according to the Peppas–Sahlin model. In vitro swelling and release experiments for prepared IPECs

It can be concluded that investigated polycomplexes are prospects for further evaluation as carriers for gastroretentive bioadhesive systems.

Supplementary Materials: It can be downloaded at: <https://www.mdpi.com/article/10.3390/scipharm92010014/s1.figure>.

Author Contributions: D.S.G. carried out synthesis and physico-chemical characterization of interpolyelectrolyte complexes, assessment of bioadhesive properties, swelling and drug release, wrote and corrected the article. A.V.S. performed elemental analysis, mathematical modeling of drug release, wrote and corrected the article. R.I.M. was responsible for conceptualization and research methodology, as well as reviewed and corrected the article. The article was written with the participation of all co-authors. All authors have read and agreed to the published version of the manuscript.

Funding: The study was carried out with the financial support of the Russian Science Foundation (RSF) in the framework of research project No 23-15-00263 (D.S.G., A.V.S. and R.I.M.).

Institutional Review Board Statement: Not applicable.

Informed Consent Statement: Not applicable.

Data Availability Statement: Data are contained within the article.

Acknowledgments: The authors are grateful to Evonik Ind. (Darmstadt, Germany) for donating samples of Eudragit® copolymers. The authors are also grateful to Alexander Sitenkov and Shamil Nasibullin for their help in physico-chemical assessment of IPEC samples.

Conflicts of Interest: The authors declare no conflicts of interest.

References

1. Alqahtani, A.A.; Mohammed, A.A.; Fatima, F.; Ahmed, M.M. Fused Deposition Modelling 3D-Printed Gastro-Retentive Floating Device for Propranolol HCl Tablets. *Polymers* **2023**, *15*, 3554. [CrossRef]
2. Patel, M.; Shelke, S.; Shaikh, F.; Surti, N.; Panzade, P.; Panjwani, D. Gastroretentive Floating Microsponges of Mitiglinide: Design, Preparation, and Pharmacokinetic Evaluation. *J. Pharm. Innov.* **2023**, *14*, 1500–1514. [CrossRef]
3. Malladia, M.; Jukanti, R. Formulation development and evaluation of a novel bi-dependent clarithromycin gastroretentive drug delivery system using Box-Behnken design. *J. Drug Deliv. Sci. Technol.* **2016**, *35*, 134–145. [CrossRef]
4. Uboldi, M.; Melocchi, A.; Moutaharrik, S.; Palugan, L.; Cerea, M.; Foppoli, A.; Maroni, A.; Gazzaniga, A.; Zema, L. Administration strategies and smart devices for drug release in specific sites of the upper GI tract. *J. Control. Release* **2022**, *348*, 537–552. [CrossRef] [PubMed]
5. Awasthi, R.; Kulkarni, G.T. Decades of research in drug targeting to the upper gastrointestinal tract using gastroretention technologies: Where do we stand? *Drug Deliv.* **2016**, *23*, 378–394. [CrossRef] [PubMed]
6. Naseem, F.; Shah, S.U.; Rashid, S.A.; Farid, A.; Almeahadi, M.; Alghamdi, S. Metronidazole Based Floating Bioadhesive Drug Delivery System for Potential Eradication of *H. pylori*: Preparation and In Vitro Characterization. *Polym. J.* **2022**, *14*, 519. [CrossRef]
7. Sravya, V.; Suresh, K.P.; Jagannath, P.V.; Sunitha, C. Formulate gastroretentive floating bioadhesive drug delivery system of nizatidine by direct compression technique. *World J. Pharm. Sci.* **2022**, *10*, 59–73. [CrossRef]
8. Altreuter, D.H.; Kirtane, A.R.; Grant, T.; Kruger, C.; Traverso, G.; Bellinger, A.M. Changing the pill: Developments toward the promise of an ultra-long-acting gastroretentive dosage form. *Exp. Opin. Drug Deliv.* **2018**, *15*, 189–1198. [CrossRef] [PubMed]
9. Zhang, C.; Tang, J.; Liu, D.; Li, X.; Cheng, L.; Tang, X. Design and evaluation of an innovative floating and bioadhesive and multiparticulate drug delivery system based on hollow structure. *Int. J. Pharm.* **2016**, *503*, 41–55. [CrossRef]
10. Patel, K.; Chouksey, R. A Recent Advantage on Gastroretentive Drug Delivery System: An Overview. *Res. J. Pharm. Technol.* **2023**, *15*, 36–44. [CrossRef]
11. Pawar, V.K.; Kansal, S.; Asthana, S.; Chourasia, M.K. Industrial perspective of gastroretentive drug delivery systems: Physico-chemical, biopharmaceutical, technological and regulatory consideration. *Exp. Opin. Drug Deliv.* **2012**, *9*, 551–565. [CrossRef] [PubMed]
12. Tripathi, J.; Thapa, P.; Maharjan, R.; Jeong, S.H. Current State and Future Perspectives on Gastroretentive Drug Delivery Systems. *Pharmaceutics* **2019**, *11*, 193. [CrossRef] [PubMed]
13. Singh, B.; Sharma, V.; Mohan, M.; Rohit, Sharma, P.; Ram, K. Design of ciprofloxacin impregnated dietary fiber psyllium-moringa gum-alginate network hydrogels via green approach for use in gastro-retentive drug delivery system. *Bioact. Carbohydr. Diet. Fiber* **2023**, *29*, 100345. [CrossRef]
14. Farhaj, S.; Conway, B.R.; Ghori, M.U. Nanofibres in Drug Delivery Applications. *Fibers* **2023**, *11*, 21. [CrossRef]

15. Das, S.; Kaur, S.; Rai, V.K. Gastro-retentive drug delivery systems: A recent update on clinical pertinence and drug delivery. *Drug Deliv. Transl. Res.* **2021**, *11*, 1849–1877. [[CrossRef](#)] [[PubMed](#)]
16. Pal, R.; Pandey, P.; Nogai, L.; Arushi; Anand, A.; Suthar, P.; Keskar, M.S.; Kumar, V. The Future Perspectives and Novel Approach on Gastro Retentive Drug Delivery System (GRDDS) with Current State. *Can. J. Clin. Pharmacol.* **2023**, *30*, 594–613. [[CrossRef](#)]
17. Zhu, X.; Qi, X.; Wu, Z.; Zhang, Z.; Xing, J.; Li, X. Preparation of multiple-unit floating-bioadhesive cooperative minitables for improving the oral bioavailability of famotidine in rats. *Drug Deliv.* **2014**, *21*, 459–466. [[CrossRef](#)]
18. Darbasizadeha, B.; Motasadizadehb, H.; Foroughi-Niac, B.; Farhadnejad, H. Tripolyphosphate-crosslinked chitosan/poly (ethylene oxide) electrospun nanofibrous mats as a floating gastro-retentive delivery system for ranitidine hydrochloride. *J. Pharm. Biomed. Anal.* **2018**, *153*, 63–75. [[CrossRef](#)]
19. Meng, S.; Wang, S.; Piao, M.G. Prescription Optimization of Gastroretentive Furosemide Hollow-Bioadhesive Microspheres via Box-Behnken Design: In Vitro Characterization and in Vivo Evaluation. *J. Drug Deliv. Sci. Technol.* **2022**, *70*, 103235. [[CrossRef](#)]
20. Ngwuluka, N.C.; Choonara, Y.E.; Modi, G.; du Toit, L.C.; Kumar, P.; Ndesendo, V.M.K.; Pillay, V.A. Design of an Interpolyelectrolyte Gastroretentive Matrix for the Site-Specific Zero-Order Delivery of Levodopa in Parkinson's Disease. *AAPS PharmSciTech* **2013**, *14*, 605–619. [[CrossRef](#)]
21. Gallardo, D.; Skalsky, B.; Kleinebudde, P. Controlled release solid dosage forms using combinations of (meth)acrylate copolymer. *Pharm. Dev. Technol.* **2008**, *13*, 413–423. [[CrossRef](#)]
22. Siepmann, F.; Siepmann, J.; Walther, M.; MacRae, R.J.; Bodmeier, R. Polymer blends for controlled release coatings. *J. Control. Release* **2008**, *125*, 1–15. [[CrossRef](#)]
23. Mustafin, R.I. Interpolymer combinations of chemically complementary grades of Eudragit copolymers: A new direction in the design of peroral solid dosage forms of drug delivery systems with controlled release (review). *Pharm. Chem. J.* **2011**, *45*, 285–295. [[CrossRef](#)]
24. Moustafine, R.I. Role of macromolecular interactions of pharmaceutically acceptable polymers in functioning oral drug delivery systems. *Russ. J. Gen. Chem.* **2014**, *84*, 364–367. [[CrossRef](#)]
25. Moustafine, R.I.; Kabanova, T.V.; Kemenova, V.A.; Van den Mooter, G. Characteristics of interpolyelectrolyte complexes of Eudragit E100 with Eudragit L100. *J. Control. Release* **2005**, *103*, 191–198. [[CrossRef](#)]
26. Moustafine, R.I.; Bukhovets, A.V.; Sitenkov, A.Y.; Kemenova, V.A.; Rombaut, P.; Van den Mooter, G. Eudragit® E PO as a complementary material for designing oral drug delivery systems with controlled release properties: Comparative evaluation of new interpolyelectrolyte complexes with countercharged Eudragit® L100 copolymers. *Mol. Pharm.* **2013**, *10*, 2630–2641. [[CrossRef](#)]
27. Sauer, D.; McGinity, J.W. Properties of theophylline tablets dry powder coated with Eudragit E PO and Eudragit L 100–55. *Pharm. Dev. Technol.* **2009**, *16*, 632–641. [[CrossRef](#)]
28. Obeidat, W.M.; Abu Znait, A.H.; Sallam, A.A. Novel combination of anionic and cationic polymethacrylate polymers for sustained release tablet preparation. *Drug Dev. Ind. Pharm.* **2008**, *34*, 650–660. [[CrossRef](#)] [[PubMed](#)]
29. Obeidat, W.M.; Abu Znait, A.H.; Sallam, A.A. Sustained release tablets containing soluble polymethacrylates: Comparison with tableted polymethacrylate IPEC polymers. *AAPS PharmSciTech* **2010**, *11*, 54–63. [[CrossRef](#)] [[PubMed](#)]
30. Bani-Jaber, A.H.; Alkawareek, M.J.; Al-Gousous, J.J.; Abu Helwa, A.Y. Floating and sustained-release characteristics of effervescent tablets prepared with a mixed matrix of Eudragit L100-55 and Eudragit E PO. *Chem. Pharm. Bull.* **2011**, *59*, 155–160. [[CrossRef](#)] [[PubMed](#)]
31. Bani-Jaber, A.H.; Al-Aani, L.; Alkhatib, H.; Al-Khalidi, B. Prolonged intragastric drug delivery mediated by Eudragit E carageenan polyelectrolyte matrix tablets. *AAPS PharmSciTech* **2011**, *12*, 354–361. [[CrossRef](#)] [[PubMed](#)]
32. Quinteros, D.A.; Manzo, R.H.; Allemandi, D.A. Interaction between Eudragit E100 and anionic drugs: Addition of anionic polyelectrolytes and their influence on drug release performance. *J. Pharm. Sci.* **2011**, *100*, 4664–4673. [[CrossRef](#)] [[PubMed](#)]
33. Wulff, R.; Leopold, C.S. Coatings from blends of Eudragit® RL and L55: A novel approach in pH-controlled drug release. *Int. J. Pharm.* **2014**, *476*, 78–87. [[CrossRef](#)] [[PubMed](#)]
34. Wulff, R.; Leopold, C.S. Coatings of Eudragit® RL and L55 blends: Investigations on the drug release mechanism. *AAPS PharmSciTech* **2016**, *17*, 493–503. [[CrossRef](#)]
35. Garciaa, M.C.; Martinell, M.; Ponced, N.E.; Sanmarcoe, L.M.; Aokie, M.P.; Manzo, R.H.; Jimenez-Kairuz, A.F. Multi-kinetic release of benzimidazole-loaded multiparticulate drug delivery systems based on polymethacrylate interpolyelectrolyte complexes. *Eur. J. Pharm. Sci.* **2018**, *120*, 107–122. [[CrossRef](#)] [[PubMed](#)]
36. Sester, C.; Ofriidam, F.; Lebaz, N.; Gagnière, E.; Mangin, D.; Elaissari, A. pH-Sensitive methacrylic acid–methyl methacrylate copolymer Eudragit L100 and dimethylaminoethyl methacrylate, butyl methacrylate, and methyl methacrylate tri-copolymer Eudragit E100. *Polym. Adv. Technol.* **2020**, *31*, 440–450. [[CrossRef](#)]
37. Bukhovets, A.V.; Fotaki, N.; Khutoryanskiy, V.V.; Moustafine, R.I. Interpolymer complexes of Eudragit® copolymers as novel carriers for colon-specific drug delivery. *Polymers* **2020**, *12*, 1459. [[CrossRef](#)] [[PubMed](#)]
38. Gordeeva, D.S.; Sitenkova, A.V.; Moustafine, R.I. Interpolyelectrolyte complexes based on Eudragit® copolymers as carriers for bioadhesive gastroretentive metronidazole delivery system. *Drug Dev. Reg.* **2020**, *9*, 72–76. [[CrossRef](#)]
39. Lankalapalli, S.; Kolapalli, V.R.M. Polyelectrolyte complexes: A review of their applicability in drug delivery technology. *Ind. J. Pharm. Sci.* **2009**, *71*, 481–487. [[CrossRef](#)]

40. De Robertis, S.; Bonferoni, M.C.; Elviri, L.; Sandri, G.; Caramella, C.; Bettini, R. Advances in oral controlled drug delivery: The role of drug—Polymer and interpolymer non-covalent interactions. *Exp. Opin. Drug Deliv.* **2015**, *12*, 441–453. [[CrossRef](#)]
41. Porfiryeva, N.N.; Nasibullin, S.F.; Abdullina, S.G.; Tukhbatullina, I.K.; Moustafine, R.I.; Khutoryanskiy, V.V. Acrylated Eudragit® E PO as a novel polymeric excipient with enhanced mucoadhesive properties for application in nasal drug delivery. *Int. J. Pharm.* **2019**, *562*, 241–248. [[CrossRef](#)] [[PubMed](#)]
42. Porfiryeva, N.N.; Semina, I.I.; Salakhov, I.A.; Moustafine, R.I.; Khutoryanskiy, V.V. Mucoadhesive and mucus-penetrating interpolyelectrolyte complexes for nose-to-brain drug delivery. *Nanomed. NBM* **2021**, *37*, 102432. [[CrossRef](#)] [[PubMed](#)]
43. Shin, S.; Kim, T.H.; Jeong, S.W.; Chung, S.E.; Lee, D.Y.; Kim, D.H.; Shin, B.S. Development of a gastroretentive delivery system for acyclovir by 3D printing technology and its in vivo pharmacokinetic evaluation in Beagle dogs. *PLoS ONE* **2017**, *14*, e0216875. [[CrossRef](#)]
44. Farshforoush, P.; Ghanbarzadeh, S.; Gpganian, A.M.; Hamishehkar, H. Novel metronidazole-loaded hydrogel as a gastroretentive drug delivery system. *Iran. Polym. J.* **2017**, *26*, 895–901. [[CrossRef](#)]
45. Peppas, N.; Sahlin, J. A simple equation for the description of solute release. III. Coupling of diffusion and relaxation. *Int. J. Pharm.* **1989**, *57*, 169–172. [[CrossRef](#)]
46. Zhang, Y.; Huo, M.; Zhou, J.; Zhou, A.; Li, W.; Yao, C.; Xie, S. DDSolver: An Add-In Program for Modeling and Comparison of Drug Dissolution Profiles. *AAPS J.* **2010**, *3*, 263–271. [[CrossRef](#)] [[PubMed](#)]
47. Boddupalli, B.M.; Mohammed, Z.N.; Nath, R.A.; Banji, D. Mucoadhesive drug delivery system: An overview. *J. Adv. Pharm. Technol. Res.* **2010**, *1*, 381–387. [[CrossRef](#)]
48. Zhang, S.; Fang, M.; Zhang, Q.; Li, X.; Zhang, T. Evaluating the bioequivalence of metronidazole tablets and analyzing the effect of *in vitro* dissolution on *in vivo* absorption based on PBPK modeling. *Drug Dev. Ind. Pharm.* **2019**, *45*, 1646–1653. [[CrossRef](#)]
49. Sulistiawati; Dwipayanti, K.S.; Azhar, M.; Rahman, L.; Pakki, E.; Himawan, A.; Permana, A.D. Enhanced skin localization of metronidazole using solid lipid microparticles incorporated into polymeric hydrogels for potential improved of rosacea treatment: An ex vivo proof of concept investigation. *Int. J. Pharm.* **2022**, *628*, 122327. [[CrossRef](#)]
50. Wu, F.; Cristofolletti, R.; Zhao, L.; Rostami-Hodjegan, A. Scientific considerations to move towards biowaiver for biopharmaceutical classification system classIII drugs: How modeling and simulation can help. *Biopharm. Drug Dispos.* **2021**, *42*, 118–127. [[CrossRef](#)]
51. Mady, O.I.; Osman, M.A.; Sarhan, N.I.; Shatla, A.A.; Haggag, Y.A. Bioavailability enhancement of acyclovir by honey: Analytical and histological evidence. *J. Drug Deliv. Sci. Technol.* **2023**, *80*, 104155. [[CrossRef](#)]
52. Filippova, N.I.; Teslev, A.A. Application of mathematical modeling in the evaluation of in vitro drug release. *Drug Dev. Reg.* **2017**, *4*, 218–226.
53. Unagollaa, J.M.; Jayasuriya, A.C. Drug transport mechanisms and in vitro release kinetics of vancomycin encapsulated chitosan-alginate polyelectrolyte microparticles as a controlled drug delivery system. *Eur. J. Pharm. Sci.* **2018**, *114*, 199–209. [[CrossRef](#)] [[PubMed](#)]

Disclaimer/Publisher’s Note: The statements, opinions and data contained in all publications are solely those of the individual author(s) and contributor(s) and not of MDPI and/or the editor(s). MDPI and/or the editor(s) disclaim responsibility for any injury to people or property resulting from any ideas, methods, instructions or products referred to in the content.